A Comparative Numerical Analysis for Vortex Generation on Different Geometries

Shahadat Hossain Zehad, Sadman Al Faiyaz, Irfan Ahmed and Ahmed Masruk Raihan

***Abstract*—Demand for renewable energy is escalating in the present world where power generation through generating vortex which is the whirling mass of fluid plays a crucial role in being harmless for the environment. This study is composed of analyzing different structures of vortex chamber by implementing several conditions for extracting the finest vortex generation that will be efficient enough to move the runner blades for the production of electricity. Two different geometries of vortex chamber of different diameters along with channel with a contraction section are carried out for simulation through ANSYS CFD after modeling in CAD for the comparison for most befitting vortex generation is obtained by differentiating through pressure, velocity, swirling strength, and from different diameters of the vortex chamber.**

***Index Terms*— Vorticity, vortex, computational fluid dynamics (CFD), swirling strength, pressure, velocity**

I. INTRODUCTION

HYDRO-POWER which is one of the major vital sources of renewable energy bears a great impact in the field of power generation. As vorticity is an advantageous medium for harnessing the power and for being spotless by moving the flow of water in a circular motion, micro-hydropower plants are constructed in such areas where the low head of water is available. Some of the investigations have gone through regarding gravitational water vortex power generation. For Example, Wanchat and Suntivarakorn (2011) reveal the most beneficial layout for a gravitational water vortex pool in a cylindrically shaped reservoir with an outlet at the center of the bottom. Comparably, Li et al., Mih, and Chen et al. described the relation of inverse proportionality between tangential velocity and water vortex radius. Mulligan and Casserly also explained that the most favorable strength of vorticity for low to high head sites where the diameter of the basin outlet section to the diameter to the basin ratio ranges from 14 to 18% [1]. As several types of research have been carried out by comparing vorticity by changing multiple dimensions of the vortex chamber, this study will be the comparison of two vortex chamber geometries undergoing through various conditions employing simulation from where the best vorticity can be picked up observing the effects of pressure, velocity, and swirling strength which has enough capability for power generation by changing the conditions of height and the diameter of the chamber.

Manuscript received January 26, 2021; revised April 28, 2021.

Shahadat Hossain Zehad is a student at the Department of Mechanical Engineering, Bangladesh Army University of Science and Technology, Saidpur 5311, Bangladesh (phone: +880 17 7517 8402; e-mail: shahadathossain01798@gmail.com).

Sadman Al Faiyaz is a student at the Department of Mechanical Engineering, Bangladesh Army University of Science and Technology, Saidpur 5311, Bangladesh (e-mail: alfaiyaz22@gmail.com).

Irfan Ahmed is an Associate Professor and Head of the Department of Mechanical Engineering, Bangladesh Army University of Science and Technology, Saidpur 5311, Bangladesh (e-mail: irfan_ahmed@baust.edu.bd).

Ahmed Masruk Raihan is a student at the Department of Mechanical Engineering, Bangladesh Army University of Science and Technology, Saidpur 5311, Bangladesh (e-mail: ahmedraihan753@gmail.com).

II. METHODOLOGY

A. Description of Designed Model

Two different structure of vortex chamber has been designed for analyzing the vorticity. The design includes two vortex chambers having two different chamber diameters and heights with outlets attached with respective channels having a section where contraction has been made. The major change in design was brought in the diameter and the height of the vortex chamber for the second model by keeping the rest of the geometries the same.

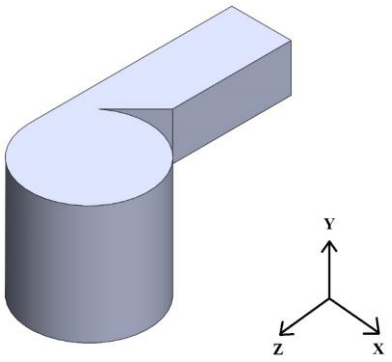

Fig 1 3D CAD Model for Case-I

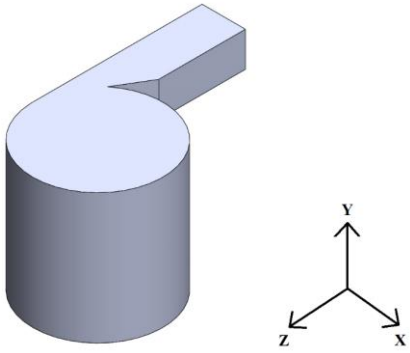

Fig 2 3D CAD Model for Case-II

Fig 1 and Fig 2 illustrates the designed model for Case-I and Case-II along with the coordinates where the origin point was set at the bottom center for Case-I and from the origin point 0.5m extra portion was extruded for Case-II

ISBN: 978-988-14049-2-3
ISSN: 2078-0958 (Print); ISSN: 2078-0966 (Online)

TABLE I
VALUES OF TWO GEOMETRIES

Section of Vortex Chamber	Model for Case-I Value (m)	Model for Case-II Value (m)
Chamber Diameter	1	1.5
Chamber Height	1	1.5
Channel Inlet Height	0.4	0.4
Channel Inlet Width	0.5	0.5
Diameter of the Outlet	0.15	0.15

B. *Governing Equations and Mathematical Modeling*

For acquiring the vorticity, the governing equations which could be viscous, incompressible, steady, and as well as a turbulent flow that can be contended as the continuity equation and also the Navier Stokes equation related to the coordinates of a cylinder which is placed as [2][3]

$$\frac{\partial V_r}{\partial r}+\frac{\partial V_z}{\partial z}+\frac{V_r}{r}=0 \quad (1)$$

$$\partial V_r\frac{\partial V_\theta}{\partial r}+VZ\frac{\partial V_\theta}{\partial z}-\frac{V_rV_\theta}{r}=v\left(\frac{\partial^2 V_\theta}{\partial r^2}+\frac{\partial V_\theta}{r\,\partial r}-\frac{V_\theta}{r^2}+\frac{\partial^2 V_\theta}{\partial z^2}\right) \quad (2)$$

$$V_r\frac{\partial V_r}{\partial r}+VZ\frac{\partial V_r}{\partial z}-\frac{V_\theta^2}{r}+\frac{\partial \rho}{\rho\,\partial r}=v\left(\frac{\partial^2 V_r}{\partial r^2}+\frac{\partial V_r}{r\,\partial r}-\frac{V_r}{r^2}+\frac{\partial^2 V_r}{\partial z^2}\right) \quad (3)$$

$$\partial V_r\frac{\partial V_z}{\partial r}+VZ\frac{\partial V_z}{\partial z}+\frac{\partial \rho}{\rho\,\partial z}=g+v\left(\frac{\partial^2 V_z}{\partial r^2}+\frac{\partial V_z}{r\,\partial r}+\frac{\partial^2 V_r}{\partial z^2}\right) \quad (4)$$

As it is very difficult to crack through the above equations analytically, ANSYS CFD Fluent was used for the solution of the given equations [4].

C. *Numerical Analysis*

The meshing of the two models has been done as fine as possible. The models were meshed with Tetrahedrons with an element number of 507476 for Case-I and 506886 for Case-II respectively with an aspect ratio of 1.94 and skewness of 0.27 for both cases.

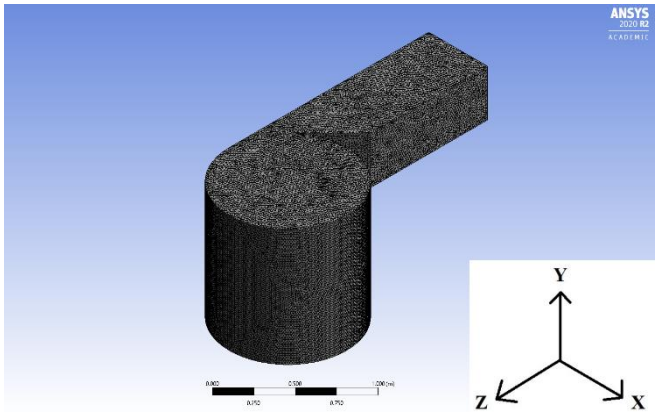

Fig 3 Meshing Model for Case-I

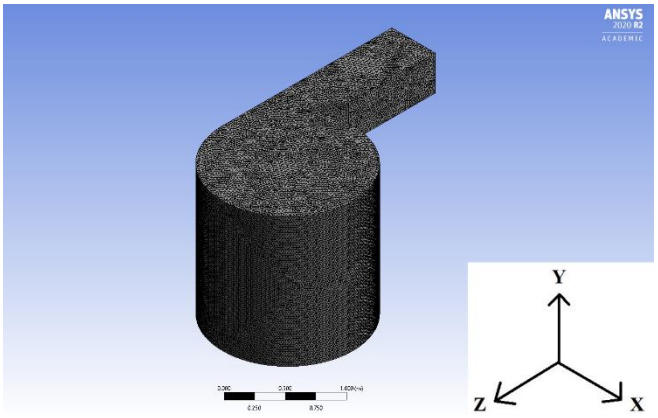

Fig 4 Meshing Model for Case-II

The pressure loss coefficient that specifies pressure loss of a certain system or of a part of a system has been calculated for both of the cases where the value of the finest mesh has been found 1.38 for Case-I and 0.93 for Case-II. The range of asymptotic convergence for Case-I was obtained 1.04 with an error of 0.11 and for Case-II the asymptotic convergence range was 1.02 with an error of 0.13 that reveals the solutions are competent within the range of asymptotic convergence [5].

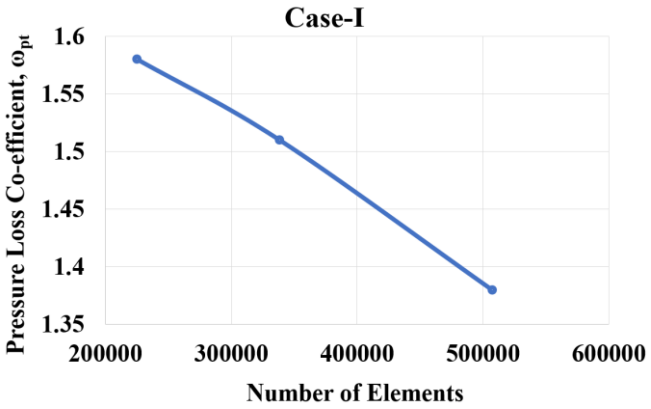

Fig 5 Pressure Loss Coefficient Versus Number of the Cells for Case-I

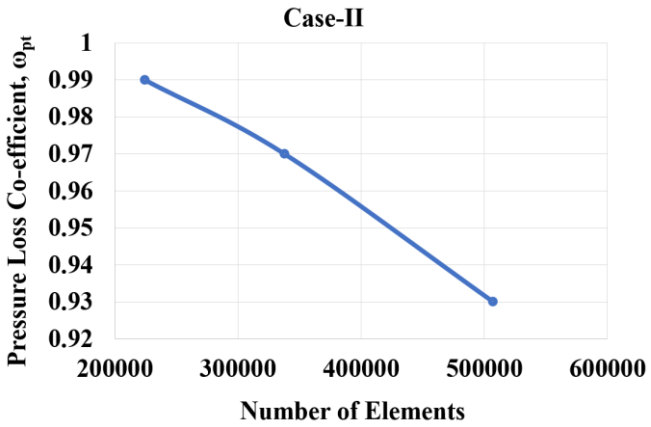

Fig 6 Pressure Loss Coefficient Versus Number of the Cells for Case-II

The simulation was executed using the SIMPLE method. The water flow was let to be run at a steady state by taking the viscous model of k-epsilon at a standard model. The incoming velocity from the channel that is the inlet was taken velocity inlet at 1.8 m/s and outlet as pressure outlet taking the gauge pressure at 0 Pa. 5000 iterations were set at residual convergence condition of 1e-4 for both cases.

ISBN: 978-988-14049-2-3
ISSN: 2078-0958 (Print); ISSN: 2078-0966 (Online)

III. RESULTS AND DISCUSSIONS

A. *Velocity Streamlines*

Fig 7 and Fig 8 show the velocity stream paths of the vortex chamber for Case-I and Case-II where the flow of water gets into the vortex chamber from the channel by getting contracted at the contraction section. The streamlines of water circulating spirally inside the chamber and drives out through the outlet section. Between the two cases, Case-I has acquired more velocity in the vortex chamber compared to Case-II as the radial flow of water gains more velocity for Case-I for having less height and diameter concerning Case-II where the color scale indicates the magnitude of velocity.

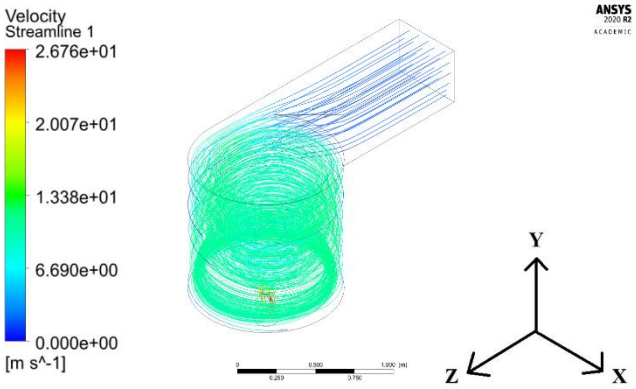

Fig 7 Velocity Streamlines for Case-I

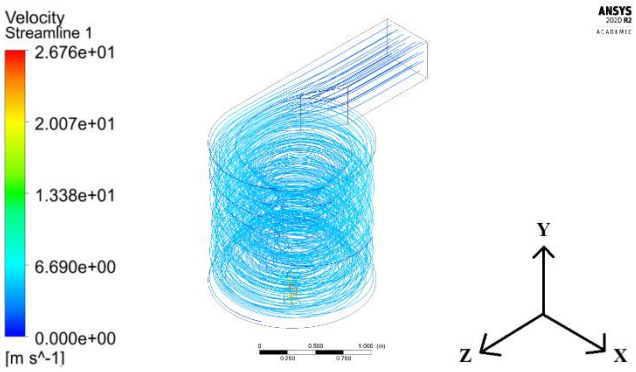

Fig 8 Velocity Streamlines for Case-II

B. *Effect on Velocity*

In Fig 9 and Fig 10, the velocity contours of the two vortex chambers are shown from where the velocity inside the chamber except the core formation of air for Case-I is more than the velocity inside the chamber for Case-II. The angle 0^0 at the XY plane section represents the plane that has been taken from the neutral position.

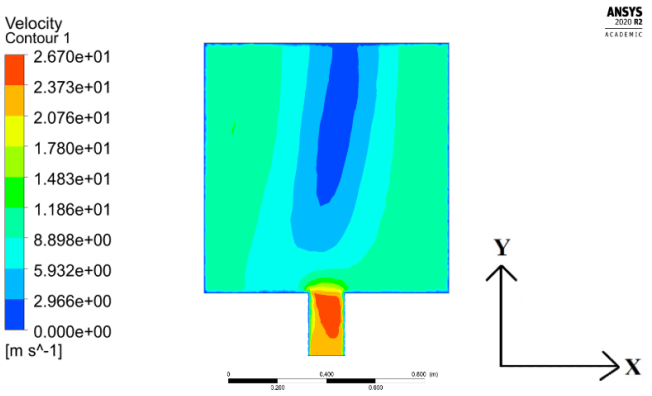

Fig 9 Velocity Contours at XY Plane in 0^0 for Case-I

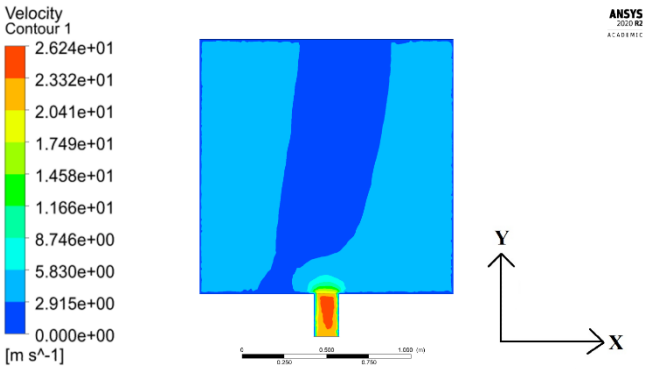

Fig 10 Velocity Contours at XY Plane in 0^0 for Case-II

From Fig 11 it has been understandably spotted that the amount of increased velocity is more for Case-I than Case-II where it has been observed that there is a slight change of velocity from 75% to 25% of the height of the chamber as there is no sudden change of geometry between those heights. After that, velocity suddenly rises due to the sudden contraction at the bottommost position of the vortex chamber.

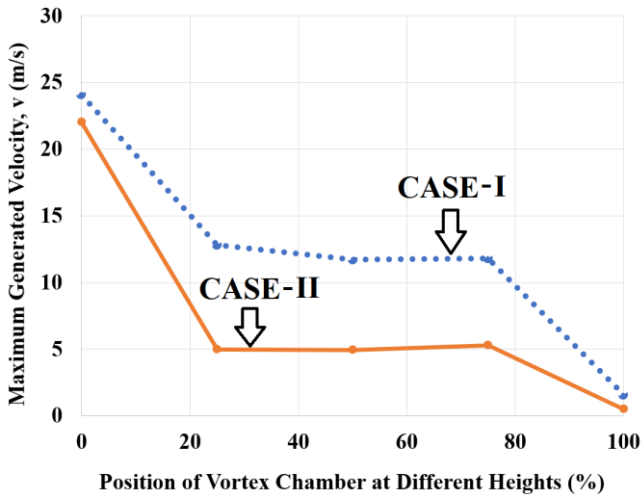

Fig 11 Velocity Curve of Vortex Chamber over Various Positions

C. *Effect on Pressure*

Pressure can be related inversely proportional to the velocity. By observing from Fig 13 to Fig 21, the contours of pressure at different spots for Case-I and Case-II which are shown bear changes in the formation of the core of vortex by the impact of pressure along with its position by taking the plane of the ZX section at different heights

ISBN: 978-988-14049-2-3
ISSN: 2078-0958 (Print); ISSN: 2078-0966 (Online)

respectively. The air core has been observed asymmetric at different heights of the plane as the core deviates from the center position.

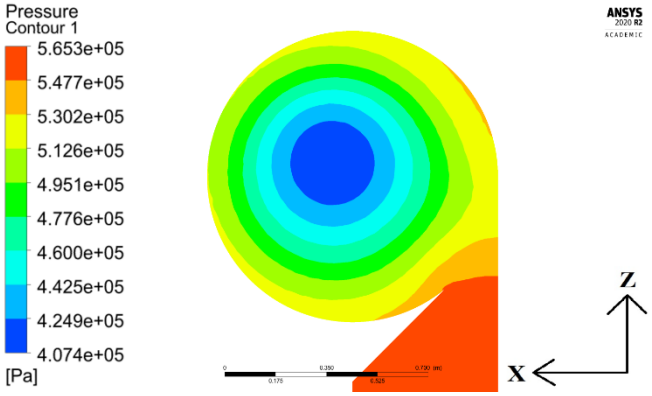

Fig 12 Pressure Contours at 100% height from the bottom of Case-I

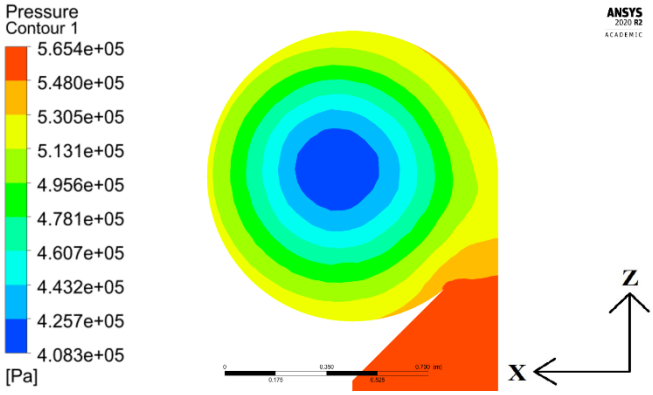

Fig 13 Pressure Contours at 75% height from the bottom of Case-I

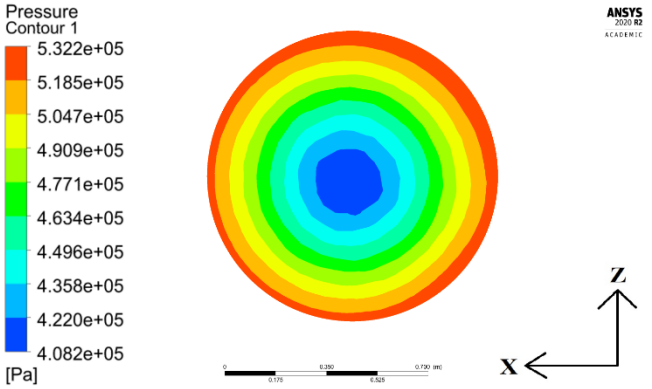

Fig 14 Pressure Contours at 50% height from the bottom of Case-I

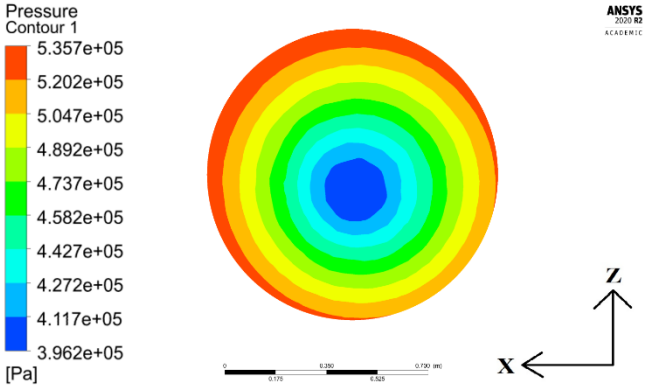

Fig 15 Pressure Contours at 25% height from the bottom of Case-I

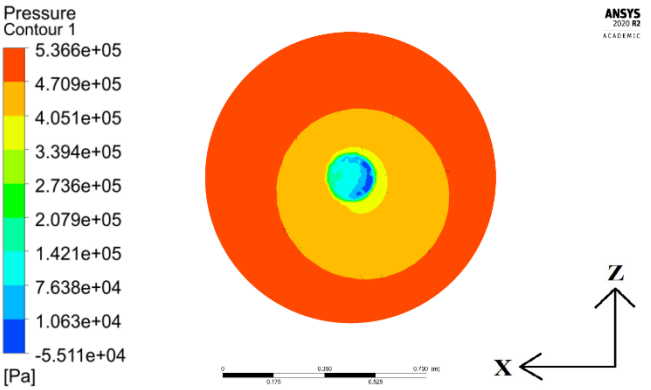

Fig 16 Pressure Contours at 0% height from the bottom of Case-I

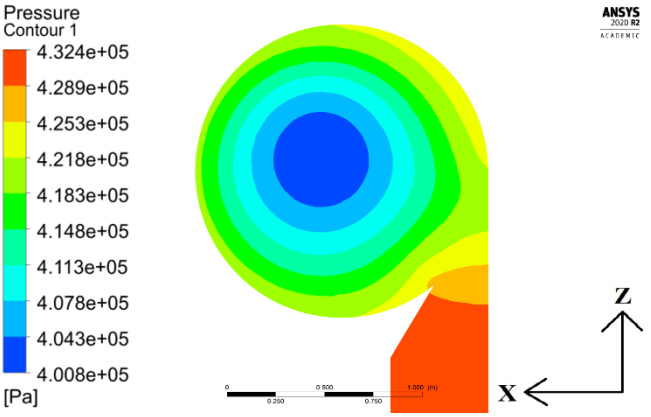

Fig 17 Pressure Contours at 100% height from the bottom of Case-II

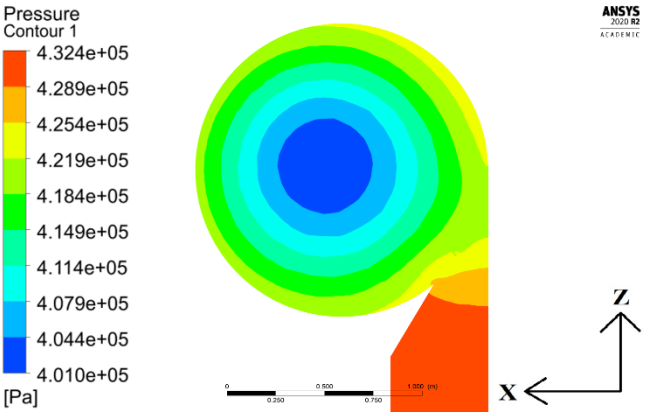

Fig 18 Pressure Contours at 75% height from the bottom of Case-II

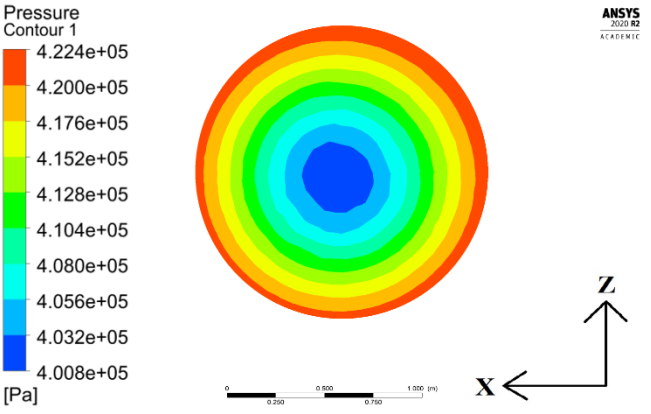

Fig 19 Pressure Contours at 50% height from the bottom of Case-II

ISBN: 978-988-14049-2-3
ISSN: 2078-0958 (Print); ISSN: 2078-0966 (Online)

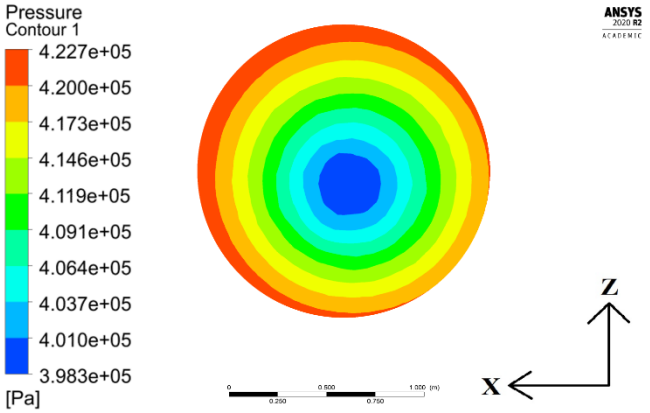

Fig 20 Pressure Contours at 25% height from the bottom of Case-II

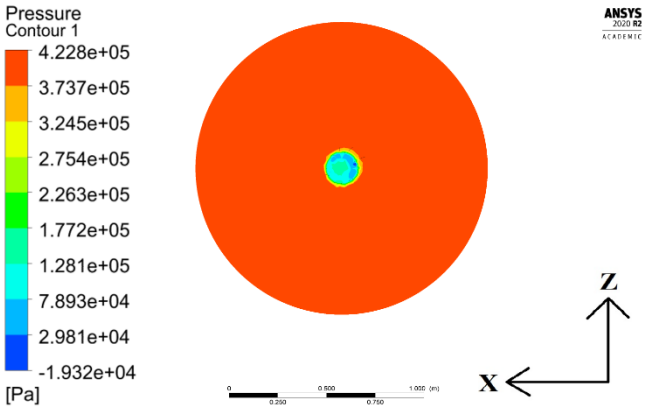

Fig 21 Pressure Contours at 0% height from the bottom of Case-II

From different models of the chamber that gives rise to vorticity which is considered as Case-I and Case-II, the pressure drop at the center of the vortex chamber for Case-I gradually decreases faster than Case-II while the flow moves towards the bottom of the chamber for vortex formation as because velocity for Case-I is greater compared to Case-II at the bottom section. As the flow of water could not acquire high velocity while moving radially towards the outlet section for being large in diameter and height for the same inlet velocity, the pressure drop slows down for Case-II compared to Case-I. Fig 22 and Fig 23 shows the pressure drop of total pressure and static pressure at the center of the vortex chamber for Case-I and Case-II at the bottom region due to sudden contraction for the outlet section where the top and bottom positions of the vortex chamber for Case-I were set at 0.8m and 0m and as for the Case-II, the top and bottom position were set at 0.8m and -0.5m respectively.

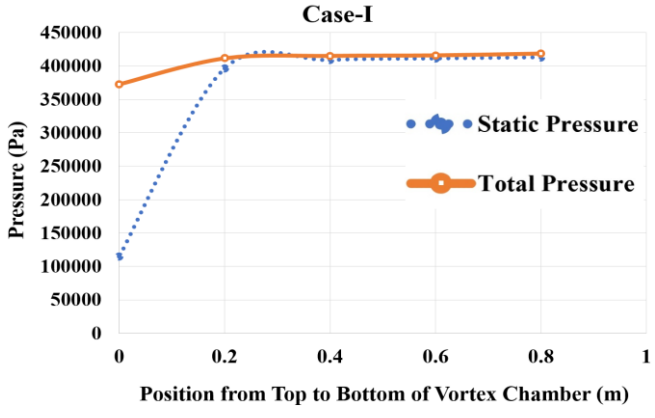

Fig 22 Pressure Curve for Case-I

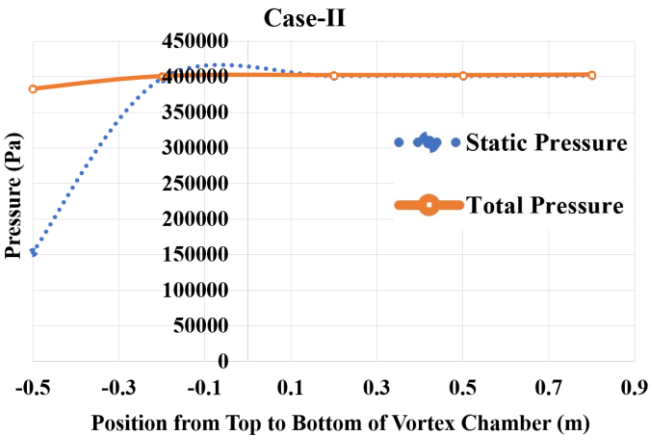

Fig 23 Pressure Curve for Case-II

D. Effect of Swirling Strength and Velocity at Vortex Core

The strength of swirl is an efficient vortex indicator in the turbulence of the wall where higher swirling strength leads to early vortex formation [6]. In Fig 24 and Fig 25 the strengths of the swirl of the two models are shown where the strength of Case-I is pretty higher than that of Case-II. As the diameter and height are greater in Case-II, the strength in Case-II lags as the circulation of water per unit area is slower compared to Case-I. Maximum swirling strength was found 30.865s^{-1} and 8.51s^{-1} for Case-I and Case-II respectively.

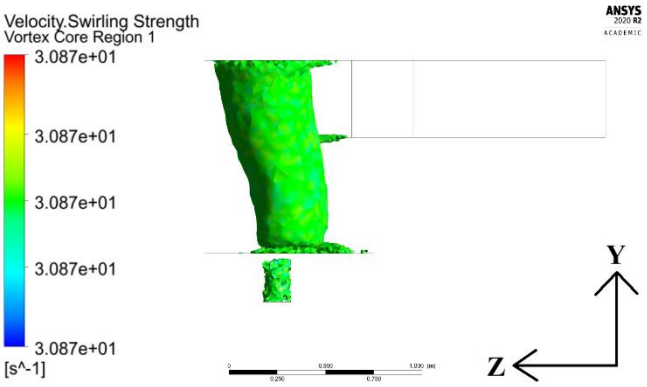

Fig 24 Swirling Strength for Case-I

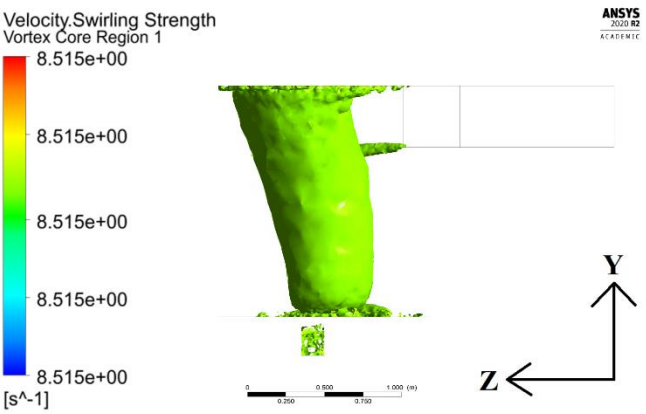

Fig 25 Swirling Strength for Case-II

ISBN: 978-988-14049-2-3
ISSN: 2078-0958 (Print); ISSN: 2078-0966 (Online)

Formation of the core of the vortex takes place due to the reason for low pressure at the bottom of the vortex chamber. [7]. The vortex core formation is less in Case-I than Case-II illustrated in Fig 26 and Fig 27 due to the change in diameter and height between the geometries. The velocity at the vortex core wall in Case-I is greater than Case-II for the same inlet flow ascribed to the swirling strength of the vortex formation. Having a larger vortex core in Case-II the strength of swirl compared to Case-I is less for not gaining the velocity of flow inside the chamber that can be noted down from the velocity at air-core formation where Case-I acquires the velocity of 25.1027m/s and Case-II acquires the velocity of 23.2634m/s. Hence the formation of a vortex in Case-II has been found weaker compared to Case-I.

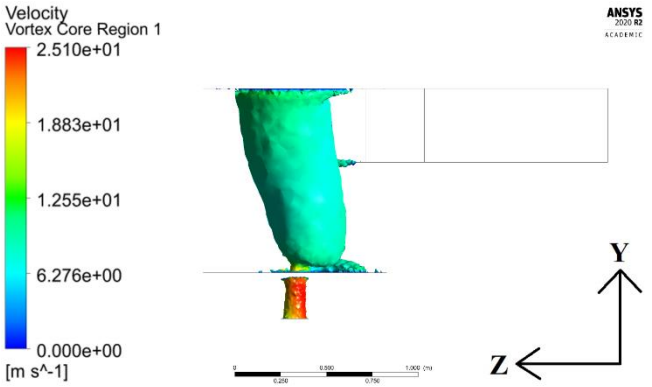

Fig 26 Velocity at Vortex-Core Formation for Case-I

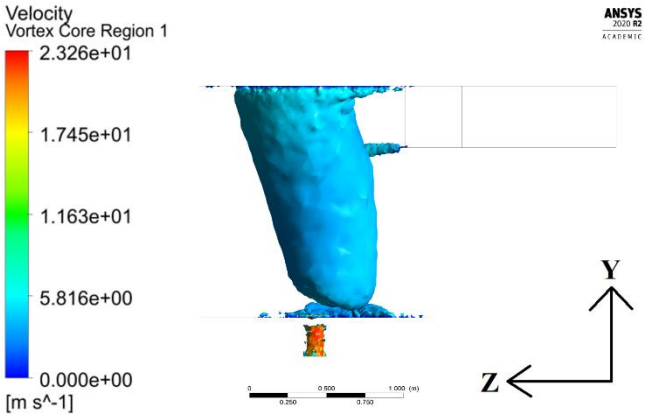

Fig 27 Velocity at Vortex-Core Formation for Case-II

IV. CONCLUSION

Comparison between two different dimensions of vortex chamber was carried out in this study to observe the best vortex formation from one of the geometry. Differentiation was made concerning velocity, pressure, swirling strength, and as well as the velocity at the vortex core formation by keeping the same aspect ratio of different dimensions where it was found that the vortex strength in Case-I is stronger than Case-II. By going through several conditions, hence the inlet velocity was the same for both cases with identical outlet section, the velocity of water for Case-II slows down at the near walls of the vortex chamber for being large in diameter and height as the circulation of water is slower than decelerates the drop of pressure and weakens the swirling strength which results in a weak vortex formation. By taking the same aspect ratio of different parameters for both Case-I and Case-II and from comparing both of the geometry, it has been observed that the aspect ratio of Case-I is suitable for strong vortex generation due to the high circulation of water flow in the vortex chamber within certain inlet velocity. This comparison study will help in selecting the suitable vortex chamber for best vortex generation according to the incoming flow of water practically where the micro-hydro power plant can be placed for extracting the energy of water and converting it for the generation of electricity.

ACKNOWLEDGMENT

The authors would firstly like to convey their special thanks of gratefulness to the Almighty Allah for giving strength and their beloved parents for giving the mental support to carry out this research and the group member of the undergraduate thesis for holding up by providing with all the facilities regarding the completion of this research.

REFERENCES

[1] J. A. Chattha, T. A. Cheema, and N. H. Khan, “Numerical investigation of basin geometries for vortex generation in a gravitational water vortex power plant,” *2017 8th International Renewable Energy Congress (IREC)*, 10.1109/IREC.2017.7926028.

[2] S. Dhakal, A. B. Timilsina, D. Fuyal, and N. Amatya, "Mathematical modeling, design optimization and experimental verification of conical basin: Gravitational water vortex power plant," *World’s Largest Hydro Conference*, Portland, 2015.

[3] Y. Wang, C. Jiang, and D. Liang, "Investigation of air-core vortex at hydraulic intakes," *9th International Conference on Hydrodynamics, Shanghai*, China, 2010.

[4] ANSYS Inc., *ANSYS Fluent Theory Guide*, Release 15.0 November 2013, E-Book Available: http://www.ansys.com.

[5] Roache, P.J., K. Ghia, and F. White, "Editorial Policy Statement on the Control of Numerical Accuracy," *ASME Journal of Fluids Engineering*, Vol. 108, No. 1., March 1986, p. 2.

[6] M. Cheng, J. Lou, and T. T. Lim, “Vortex ring with swirl: A numerical study,” *Physics of Fluids*, 22, 097101 (2010); doi: 10.1063/1.3478976.

[7] Gupta. R., Kaulaskar, M. D., Kumar, V., Sripriya, R., Meikap, B. C., and Chakraborty, S. (2008), “Studies on the understanding mechanism of air core and vortex formation in a hydrocyclone.” *Chemical Engineering Journal*, 144(2), 153–166. doi:10.1016/j.cej.2008.01.010.